SAND99-0376C

Characterization of a MEMS Accelerometer for Inertial Navigation Applications

R. D. Kinney, Sr.
Sandia National Laboratories
Albuquerque, NM 87185

Abstract

Inertial MEMS sensors such as accelerometers and angular rotation sensing devices continue to improve in performance as advances in design and processing are made. Present state-of-the-art accelerometers have achieved performance levels in the laboratory that are consistent with requirements for successful application in tactical weapon navigation systems. However, sensor performance parameters that are of interest to the designer of inertial navigation systems are frequently not adequately addressed by the MEMS manufacturer. This paper addresses the testing and characterization of a MEMS accelerometer from an inertial navigation perspective. The paper discusses test objectives, data reduction techniques and presents results from the test of a three-axis MEMS accelerometer conducted at Sandia National Laboratories during 1997. The test was structured to achieve visibility and characterization of the accelerometer bias and scale factor stability over time and temperature. Sandia is a multi-program laboratory operated by Sandia Corporation, a Lockheed Martin Company, for the United States Department of Energy under contract DE-AC04-94AL85000.

Introduction

Performance of MEMS inertial sensors continues to improve as design and fabrication advancements are achieved and this clearly enhances the attractiveness of these devices for application in low–cost, low–power navigation systems. The devices could, for example, be used as components in Global Positioning System (GPS) aided navigation systems where the sensors, accelerometers and angular rate sensing devices, provide continuous data between GPS updates and during periods when the GPS signal is not available due to interference. In these systems, errors induced by the sensors are corrected periodically by GPS derived position and velocity updates, exploiting the synergism of combining the highly accurate, but slow updating GPS navigation system with the considerably less accurate, but continuous navigation solutions of an inertial navigation system. Even application of MEMS inertial sensors in unaided inertial navigation systems is feasible for host systems that operate for brief periods where sensor errors are not as significant because they have less time to propagate. An example of the latter is smart munitions for military applications which operate for brief periods but require inertial sensor input to derive orientation and guidance information.

During 1997, Sandia National Laboratories in collaboration with the Berkeley Sensor Actuator Center (BSAC) of the University of California at Berkeley fabricated a surface micromachined three–axis accelerometer designed by BSAC and described in a paper by Mark Lemkin, et. al[1]. The accelerometer was fabricated using Sandia's IMEMS process which has the capability to integrate CMOS electronics with surface micromachined structures. Sandia's interest in building the accelerometer was partly motivated by a desire for deeper insight into performance characteristics of the accelerometer and its potential for application in nuclear weapon subsystems and test instrumentation. The BSAC accelerometer design with its integrated electronics and MEMS structure was particularly attractive because of its potential for lower electrical noise and lower assembly cost. Although, the initial fabrication lot experienced processing deficiencies and was limited in operating temperature range, a small quantity of accelerometer were judged suitably functional to justify pursuing preliminary characterization testing. This paper presents the test procedures and results of tests conducted to examine the stability of accelerometer bias and scale factor.

Test Device Description

The test device is surface micromachined, force–balanced, three–axis accelerometer with integrated CMOS circuitry. Each of the three accelerometers comprises a proof mass, proof mass suspension, capacitive pickoff mechanism, electronic servo loop, and signal digitizer. Each of the three proof masses is constrained to move in a

single dimension orthogonal to the other two thus providing the input accelerations sensing along three mutually orthogonal axes, X, Y and Z.

The X and Y axis accelerometers were implemented using a comb structure in which the fingers of a compliant comb are interdigitated with fixed comb fingers to provide an output differential signal from the capacitive coupling between individual fingers. The Y–axis comb structure is about half the mass of the X–axis.

The Z axis accelerometer is implemented differently with a hinged plate as a proof mass. The proof mass forms a capacitor with the ground plane polysilicon structure of the device. A fixed reference capacitor plate was designed into the Z axis channel to provide a differential output in conjunction with the moveable plate.

The accelerometer die is shown in Figure 1.

The initial fabrication yielded two devices suitable for further characterization in Sandia's inertial sensor test facility. The Y–axis on both test devices was not functional and only the X and Z axes were characterized. Only the results of the X-axis accelerometer are reported in this paper.

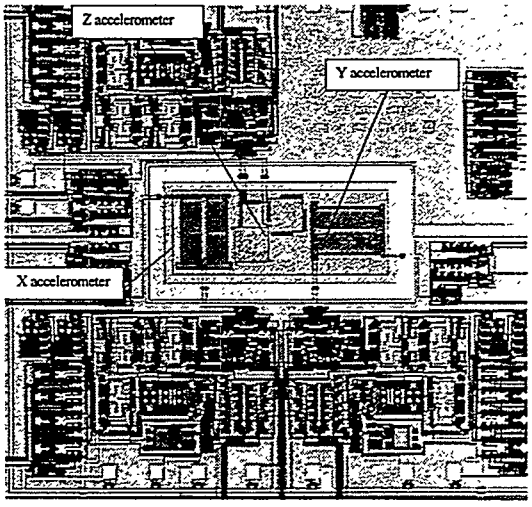

Figure 1: Three Axis MEMS Accelerometer

The electrical output of an accelerometer channel is a pulse train. The acceleration sensed by the device is contained in the pulse density of the output pulses. By design, an output or bias frequency is present even at zero input acceleration. The scale factor or density of output pulses per unit time per unit acceleration input is a function of the device clock frequency. Stability of the clock for the accelerometer directly affects accelerometer performance therefore maintaining good clock stability is essential for measuring accelerometer capability. This issue was addressed by clocking the accelerometer with a low drift, (±100 ppm from -10 to +70 °C) crystal oscillator.

Test Bed Description

The test bed for the accelerometer was configured as shown in Figure 2. Each block represents a physical entity. The accelerometer test board contains: a socket for securing the packaged accelerometer, external bias circuitry, temperature measurement circuitry, precision clock, and serial data line drivers for conveying the accelerometer output data from the indexing table via the table's slip ring assembly to a control box.

DISCLAIMER

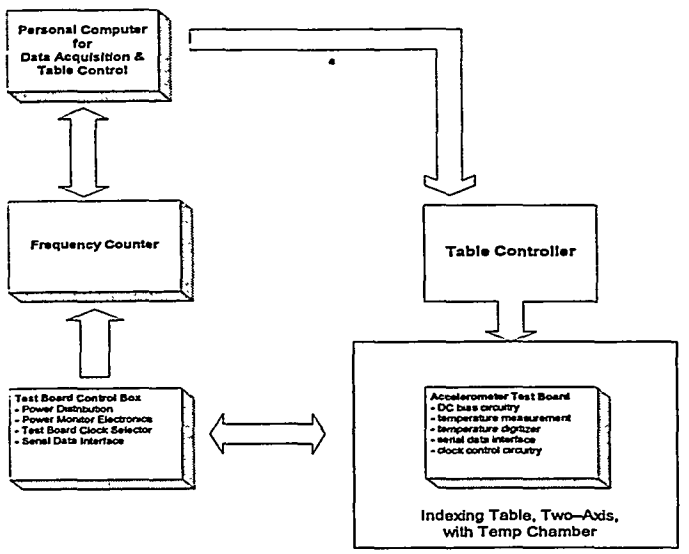

Figure 2: Test Bed Configuration

A two-axis inertial test table was used to orient the input axes of the three-axis accelerometer package relative to the local gravity vector. The surface of the test table had been leveled relative to the local gravity vector.

The accelerometer test board was mounted to a plate that interfaced with the table's mounting surface. The table provides rotational freedom around two axes. The table provided the means to orient the accelerometer input axis precisely in the local gravity field. Positioning of the table is controlled by computer.

The sketch of Figure 3 depicts the orientation of the table's inner gimbal and the test accelerometer axes for a typical test configuration. The input axes of the accelerometer are oriented to lie in the plane of the local gravity vector by a combination of table orientations and mounting of the accelerometer package on the table's inner gimbal. The table's gimbals can be positioned with an accuracy of a few arc-seconds of angle.

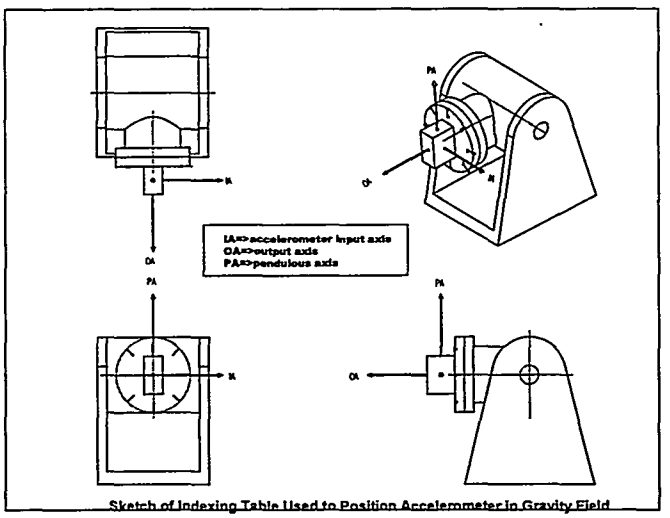

Figure 3: Orientation of Accelerometer and Test Table During Test Sequence

The table is equipped with a temperature chamber that is capable of providing a controlled ambient temperature. The chamber can either heat or cool the test device's environment and maintain the selected environment within ±0.5 degrees Celsius throughout the test period. A picture of the two–axis table with it's temperature chamber cover open is show in Figure 4.

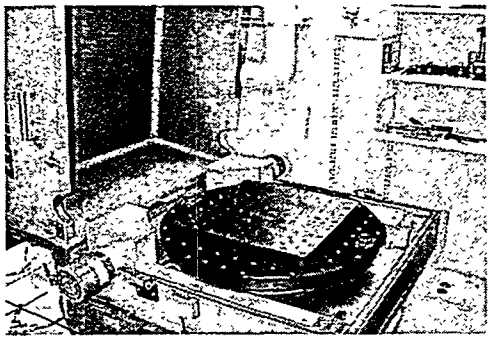

Figure 4: Two–Axis Table

Test Procedure

The basic building blocks for each axis are thus identical to that of a conventional single-axis, digital, pendulous torque balanced accelerometer. It is on this basis that the accelerometer was tested using a procedure and data reduction method similar to the procedures specified in IEEE STD 337-1972[2] and IEEE STD 530-1978[3]. These documents describe in detail a model for the accelerometer that defines an input/output function with associated error terms. The test procedure consist of observing the output of the test device to input accelerations using the Earth's gravitation field as the excitation source. Data is collected for different orientations of the devices input axis relative to the local gravity vector. The coefficients of the model terms are determined by regression analysis (least squares fit) of the test data. The magnitude of the coefficients provides insight into the error sources present in the design. Stability of the coefficients over time and temperature provides a measure of device stability.

The objectives of this first series of tests were to characterize the accelerometer under static conditions for:

1) stability of bias (zero offset) and scale factor over temperature and time
2) linearity over the range of ± one g acceleration

Dynamic testing was not performed.

The behavior of the quantized output from the accelerometer force balance loop is the same as that of a ΔΣ analog-to-digital converter. That is, the acceleration information is contained in the ones density of its output pulse stream. Typically, in ΔΣ converters, this pulse stream is the input to a finite impulse response (FIR) digital filter which is integrated with the converter's analog modulator in a single chip. The digital filter's purpose is to (1) decimate the oversampled analog modulator's output and (2) filter the high frequency noise to produce a lower frequency, high-resolution output.

The accelerometer was implemented using only the analog modulator part of a typical ΔΣ converter. It becomes the user's responsibility to provide the digital filtering and decimation, if required. This was accomplished in our test configuration by using a precision frequency counter to implement an averaging digital filter with $sin(x)/x$ filter response. This was accomplished by accumulating accelerometer output pulses over a precisely known period and dividing by the duration of the period to provide an average frequency or equivalently the ones density over the sample period. This average frequency is proportional to the input acceleration.

Resolution and frequency response of the measurement is a function of the accumulation period. For these tests, the accumulation period or gate time for the counter was set to ten seconds. For the sampling rate of the test accelerometer which is a function of the input clock frequency used to excite the circuitry, this implements a filter possessing a magnitude response as shown in Figure 5. For an accumulation period of 10 seconds, the filter

bandwidth is approximately 0.04Hz. Therefore, the measured data is high-resolution DC data. One should note that most of the noise content of the output pulse stream will also have been removed by the filtering action of our pulse accumulator filter. A more thorough examination of the accelerometer would have included a characterization of the noise content of the output over a frequency range.

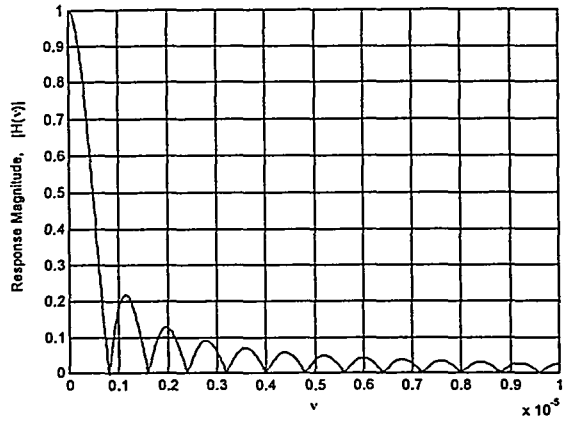

Figure 5: Plot Showing the Filtering Action of Accumulating Pulses Over a Ten Second Interval

An important characteristic of any inertial instrument is the degree to which it is susceptible to temperature changes. If the instrument's parameters change little and the changes are linear, the compensation of the instrument behavior in software is straightforward. However, if changes are large or non-linear, the effort becomes much more difficult.

Since the accelerometers failed to function at temperatures greater than about 27 degrees Celsius, the accelerometers were tested over a very limited range, but the data provides some insight into temperature sensitivity. The test devices were tested at three temperatures, 16, 21, and 27 degrees Celsius. Two parameters, bias and scale factor, were examined for changes. The limited temperature range was dictated by failure of the accelerometers to operate outside this range.

Short term stability in the context of this testing refers to the stability of accelerometer parameters between subsequent applications of power to the device. In other word, it refers to the stability of device parameters from turn-off to the next turn-on of the device for operation in the same environment. This stability is important for parameters such as bias because if the changes are random (and they usually are), it is not possible to compensate for them.

The accelerometers were tested for short-term stability by collecting data with the test device maintained in one orientation for several cycles of power turn-offs and turn-ons. The interval between successive applications of power was approximately one hour.

Data Reduction

As described earlier, the accelerometer test devices were observed for known inputs of acceleration by using the local gravity vector as the excitation source. Different values of acceleration were generated by orienting the input axes of the test devices at precisely known angles relative to the local vertical. The input acceleration to the device is thus a function of the angle between accelerometer input axis and vertical, namely, $g \cdot cosine\ (\Theta)$ where Θ is the angle between the two vectors. The output of the test device (average frequency over the sample interval, 10 seconds) plotted against the angle of the input axis of the accelerometer relative to vertical describes a cosine function. The initial data therefore is presented in the form of output frequency as a function of table angle. All DC parameters of interest can be derived from this basic data.

The data is also presented in more intuitive format by plotting indicated acceleration in terms of g (i.e. units of local gravitational acceleration) versus actual input acceleration, again in terms of g.

The error model used to describe the observed behavior of the accelerometer under the conditions described in the previous section is patterned after the model described in references 2 and 3. It was presumed that physical sources of the errors described in the references remain valid for the surface micromachined accelerometer. In addition, there may be important error sources unique to the micromachined accelerometer that are insignificant in larger scale device such as those for which the IEEE standards were addressing. These were not considered in this test series. One parameter that is common in micromachined and conventional accelerometers is temperature sensitivity. However, due to the small scale of the micromachined device, temperature is expected to play a larger role.

The error model components selected for micromachined accelerometer are:

1. bias (zero offset)
2. scale factor (gain)
3. non-linearity
4. input axis misalignment from the case reference axis about the output axis
5. cross-axis sensitivity to acceleration inputs along the input and pendulous axes
6. temperature

Misalignment of the input axis about the pendulous axis was not examined. Nor was the cross-axis sensitivity to acceleration inputs along the input and output axes. Due to the non-pendulous design of the test accelerometer, it is reasonable to expect that both these errors and error term 5 above are insignificant. That is, because acceleration is sensed in the test devices by a translation of the proof mass rather than pivoting of the proof mass about an "output" axis, there is no mechanism to give rise cross-axis sensitivity to the first order.

The equation relating average output frequency with the error model components is as follows:

$$average\,freq\ out = K_0 + K_1 * \cos(\Theta) + K_2 * \cos^2(\Theta) + K_3 * \sin(\Theta) + K_4 * \sin(2\Theta) + K_5 * \Delta T$$

where

$\Theta = accelerometer\ input\ axis\ orientation\ relative\ to\ local\ gravity\ vector$

$K_0 = Bias, Hz$

$K_1 = ScaleFactor, Hz / g$

$K_2 = g - squared\ non - linearity, Hz / g^2$

$K_3 = input\ axis\ misalignment, Hz / g$

$K_4 = cross - axis\ sensitivity, H / g^2$

$K_5 = temperature\ sensitivity, Hz / °C$

$\Delta T = change\ in\ device\ temperature\ during\ test\ from\ initial\ temperature$

The value of the coefficients of the error model were established by linear regression, i.e. by performing a least squares fit of the data which minimizes the sum of the squares of the deviation of the data from that predicted by the model. By following this procedure at several temperatures we intended to provide some insight into the temperature sensitivity of the coefficients.

Test Results

Figure 6 is an example of the data reduction as described in the preceding section. It shows the measured data, i.e., the average output frequency versus the test table orientation with a plot of the model equation versus table orientation with "best fit" coefficients.

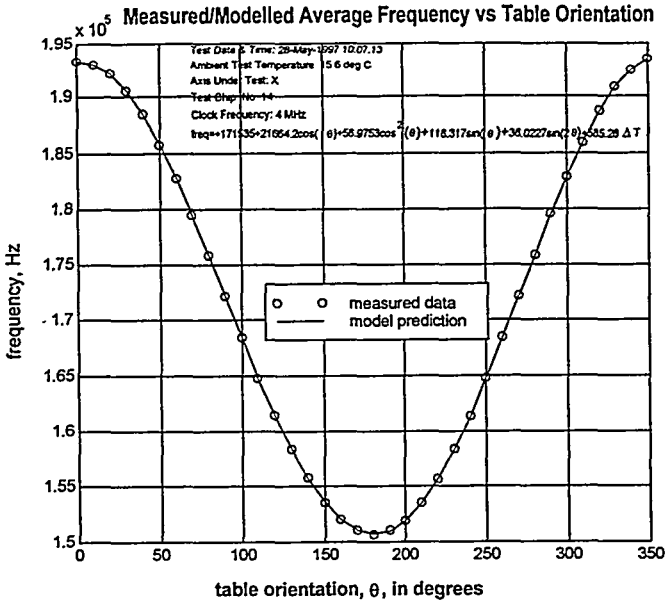

Figure 6

Figure 7 shows the frequency output from accelerometer plotted as a function of the input acceleration (in units of local gravitational acceleration, g) derived from the known orientation of the test table.

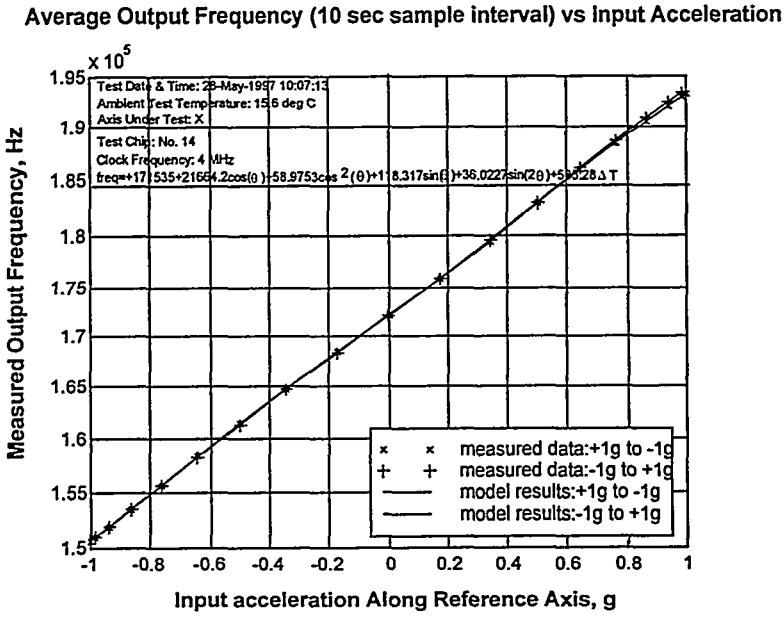

Figure 7: Comparison of Measured Data with Model Predictions

Figure 8 presents the data in terms of indicated or measured acceleration rather than frequency and Figure 9 shows the residual of the indicated acceleration after compensating the raw data using the error model. The latter provides insight into the device linearity over the range of input accelerations.

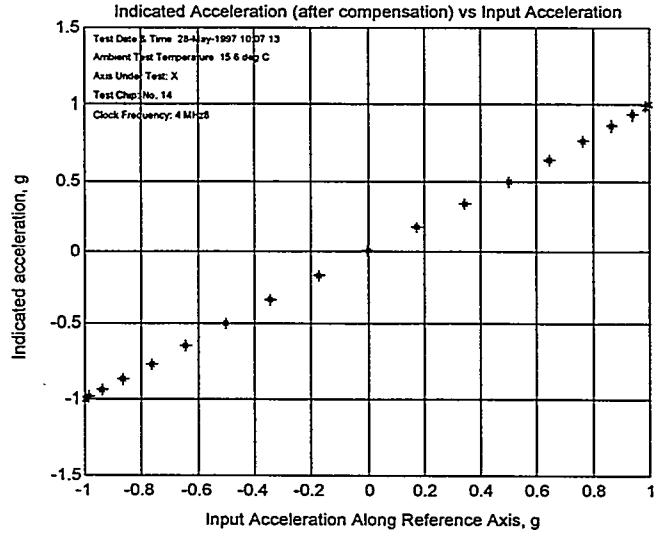

Figure 8: Compensated Data For X-Axis Accelerometer

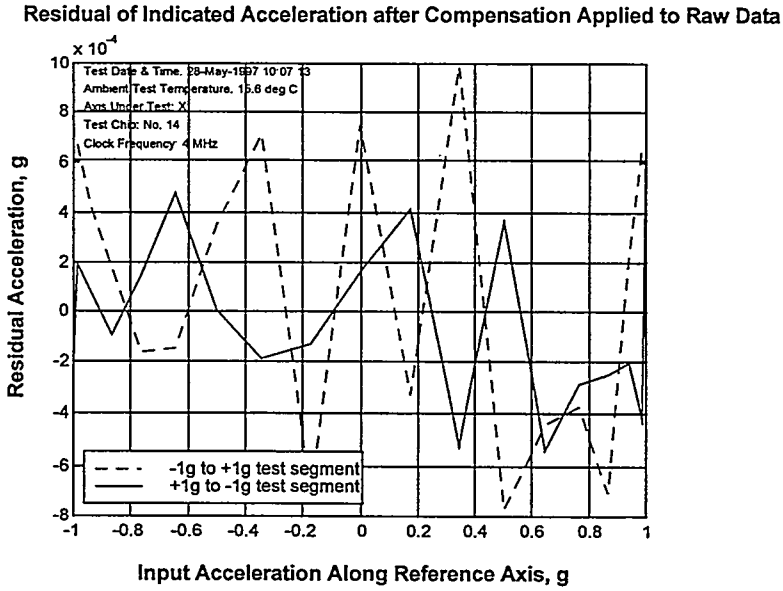

Figure 9: Residual of Model Predicted Acceleration

Table 1 is a list of typical model coefficients for the X-axis accelerometer for three runs performed on the same day at the same ambient temperature.

	Model Coefficients for Three Runs X Axis: Chip 14 @ 15.6 Deg C		
	1st Run	2nd Run	3rd Run
Bias, Hz	171548.6	171457.4	171244.9
Scale Factor, Hz/g	21655.35	21695.98	21926.83
G-sq Nonlinearity, Hz/g-sq	57.59382	66.77067	56.69872
Output Misalignment, Hz/radian	133.6652	154.3345	193.1641
Cross-axis sensitivity, Hz/g-sq	33.41831	42.1883	84.36961
Temperature sensitivity, Hz/deg C	531.2829	669.7465	1374.274

Table 1: Model Coefficients for an X-Axis Accelerometer for Three Runs

Temperature stability was examined by collecting data from the test devices at three temperatures over the range for which the accelerometers were functional. The error model coefficients were obtained for each data set and changes in bias and scale factor were calculated. The results proved to be indistinguishable from the changes observed between data sets collected at the same temperature. A qualitative assessment regarding the temperature sensitivity can not be made from this limited data.

A way of assessing bias stability is to observe its behavior between successive turn-on to turn-on sequences with the accelerometer static. Tests were conducted with the input axis of the accelerometer fixed in one orientation (typically at near zero g input) and the output measured for average frequency over a ten second interval for a period of five minutes or a total of 30 samples. Figure 10 shows a plot of the bias in g as a function of time for three runs. The transient in the bias frequency during the first few minutes is most likely due to device self heating . The longer term trend in the data also suggest a temperature related root cause However, the variation of the bias between runs is on the order of 3 milli-g. This suggests that the devices are sufficiently stable for use in tactical navigation systems.

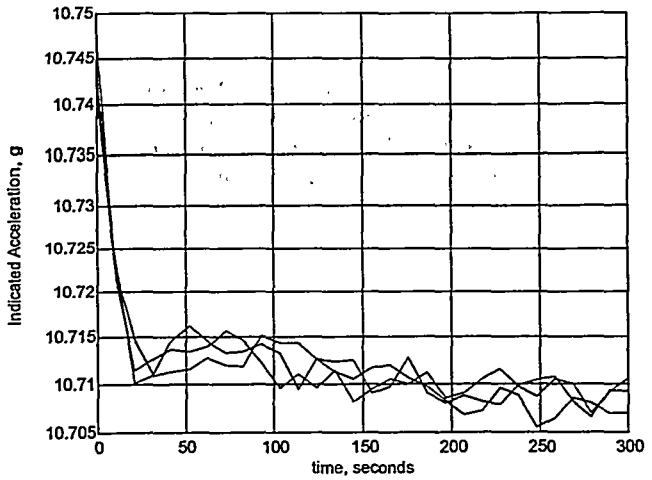

Figure 10: Behavior of X-Axis Bias For Three Successive Power-On Tests

Summary

Tests were conducted on a small sample of three axis MEMS accelerometers designed at the University of California, Berkeley and fabricated in Sandia's IMEMS process. Accelerometer bias and scale factor stability over time and temperature were examined.

Although the sample of accelerometers used in the tests was small and contained known fabrication deficiencies, the short-term stability of the X-axis accelerometer was sufficiently small to suggest that these devices could be applied in medium performance inertial measurement systems. Continued progress in design and fabrication processes is expected and therefore the prospect of achieving the performance goals established for micromachined accelerometers, namely, low cost, low power, small size, and medium performance is promising.

Operating temperature range was severely limited in the test devices and a quantitative measure of temperature sensitivity over an extended range was not achieved. However, the accelerometers clearly possess considerable temperature sensitivity and it is the author's conclusion that accurate knowledge of sensor temperature changes is essential if these devices are applied in navigation applications. Perhaps the best way to deal with this issue is to fabricate a temperature sensor into the same silicon as the accelerometer.

Acknowledgements

The author wishes to acknowledge the contribution of J. Sarsfield of Sandia who configured the test bed and performed the tests.
Also, recognition is given to the personnel of Sandia's Microelectronic Laboratory for their contribution in fabricating the test devices. In particular, J.J. Allen, J. H. Smith, and S. Montague are recognized for their contributions in the areas of MEMS design and processing technology that laid the foundation for the fabrication of the test devices.
Programmatic support was provided by Michael Callahan, Tom Hitchcock, and John Ellis of Sandia.
Michael Daily of Sandia and Mark Lemkin of Integrated Micro Instruments were particularly helpful in providing insight and assistance regarding electrical interfaces and operation of the accelerometer.

---

[1] Lemkin, M., Ortiz, M., Wongkomet, N., Boser, B.E., Smith, J.H. *A Three Axis Surface Micromachined Accelerometer,* ISSCC Digest of Technical Paper, February, 1997

[2] IEEE STD 337-1972, *IEEE Standard Specification Format Guide and Test Procedure for Linear, Single-Axis, Pendulous, Analog, Torque Balance Accelerometer*

[3] IEEE STD 530-1978, *IEEE Standard Specification Format Guide and Test Procedure for Linear, Single-Axis, Digital, Torque-Balance Accelerometer*

Sandia is a multiprogram laboratory
operated by Sandia Corporation, a
Lockheed Martin Company, for the
United States Department of Energy
under contract DE-AC04-94AL85000.